R-22 and R-410A Condensation in Flat Aluminum Multi-Channel Tubes

Nae-Hyun Kim†, Chang-Keun Min*, Ho-Jong Jung*

Department of Mechanical Engineering, University of Incheon, Incheon 402-749, Korea

**Graduate School, University of Incheon, Incheon 402-749, Korea*

Key words: Condensation, Multi-channel, Small diameter, R410A, R-22, Tube

ABSTRACT: In this study, condensation heat transfer tests were conducted in flat aluminum multi-channel tubes using R-410A, and the results are compared with those of R-22. The flat tubes have two internal geometries; one with smooth inner surface and the other with micro-fins. Data are presented for the following range of variables; vapor quality (0.1~0.9), mass flux (200~600 kg/m^{2}s) and heat flux (5~15 kW/m^2). Results show that the effect of surface tension drainage on the fin surface is more pronounced for R-22 than R-410A. The smaller Weber number of R-22 may be responsible. For the smooth tube, the heat transfer coefficient of R-410A is slightly larger than that of R-22. For the micro-fin tube, however, the trend is reversed. Possible reason is provided considering physical properties of the refrigerants. For the smooth tube, Webb's correlation predicts the data reasonably well. For the micro-fin tube, the Yang and Webb model was modified to correlate the present data. The modified model adequately predicts the data.

Nomenclature

A : heat transfer area [mm^2]
A_c : cross-sectional flow area [mm^2]
A_i : total internal surface area [mm^2]
b : thickness of the flat tube [mm]
c_p : specific heat [J/kg/K]
D_h : hydraulic diameter [mm]
e : fin height [mm]
G : mass flux [kg/m^2/s]
G_{eq} : equivalent mass flux $(=G\{(1-x)+x(\rho_l/\rho_v)^{0.5}\})$ [kg/m^2/s]
h : heat transfer coefficient [W/m^2/K]
h_f : heat transfer coefficient for finned region [W/m^2/K]
h_{sh} : heat transfer coefficient attributable to shear force [W/m^2/K]
h_{st} : heat transfer coefficient attributable to surface tension force [W/m^2/K]
h_u : heat transfer coefficient for un-finned region [W/m^2/K]
i_{fg} : latent heat of vaporization [J/kg]
k : thermal conductivity [W/m/K]
L : length of the test section [mm]
m : mass flow rate [kg/s]
Nu_{Dh} : Nusselt number based on hydraulic diameter $(=hD_h/K)$ [dimensionless]
P : pressure [N/m^2]
p : fin pitch [mm]
P_c : critical pressure [N/m^2]
Pr : Prandtl number, $\mu c_p/k$ [dimensionless]
P_{red} : reduced pressure [dimensionless]
P_w : wetted perimeter [mm]
Q : heat transfer rate [W]

† Corresponding author
Tel.: +82-32-770-8420; fax: +82-32-770-8421
E-mail address: knh0001@incheon.ac.kr

q : heat flux [W/m^2]
r_b : fin base radius [mm]
Re_{eq} : equivalent Reynolds number ($=G_{eq}D_h/\mu_l$) [dimensionless]
Re_l : Reynolds number for liquid flow
r_o : fin tip radius [mm]
S_m : length of fin profile [mm]
T : temperature [K]
t : tube wall thickness [mm]
U : overall heat transfer coefficient [W/m^2/K]
w : width of the flat tube [mm]
We : Weber number ($=G_{eq}^2D_h/\rho_l\sigma$) [dimensionless]
x : vapor quality [dimensionless]
X_{tt} : Martinelli parameter for turbulent-turbulent flow ($=\left(\frac{1-x}{x}\right)^{0.9}\left(\frac{\rho_v}{\rho_l}\right)^{0.5}\left(\frac{\mu_l}{\mu_v}\right)^{0.1}$) [dimensionless]
z : coordinate parallel to the flow [mm]

Greek symbols

γ : apex angle of the fin [deg]
μ : dynamic viscosity [kg/m/s]
ρ : density [kg/m^3]
σ : surface tension [N/m]
τ_i : wall shear stress in z direction [N/m^2]
τ_s : liquid-vapor interfacial shear stress [N/m^2]

Subscripts

ave : average
meas : measured
eq : equivalent
f : finned
i : tube-side
in : inlet
l : liquid
m : mean
o : annular-side
out : outlet
p : pre-heater
pred : predicted
r : refrigerant
sat : saturation
u : un-finned
v : vapor

1. Introduction

Fin-and-tube heat exchangers have long been used as condensers in an air-conditioning system, and rigorous efforts have been made to improve the thermal performance of the heat exchangers. These include a usage of high performance fins, and of small diameter tubes, etc. However, fin-and-tube heat exchangers have inherent short-comings such as contact resistance between fins and tubes, existence of low performance region behind tubes, etc. These short-comings may be overcome if fins and tubes are soldered, and low-profile flat tubes are used. Brazed flat-tube heat exchangers with aluminum louver fins, satisfy the requirements. Such flat-tube heat exchangers have been used as condensers of automotive air-conditioning units for more than ten years.

Cut-away views of flat tubes are shown in Fig. 1. Typical widths of flat tubes are 16 to

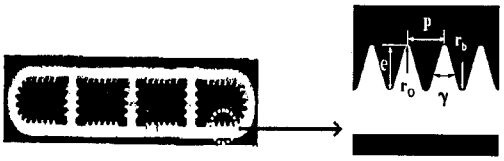

(a) Micro fin tube D_h=1.56 mm

(b) Smooth tube D_h=1.41 mm

Fig. 1 Flat extruded aluminum tubes tested in this study.

20 mm, and typical heights are 1 to 3 mm. These tubes have rectangular sub-channels of a small hydraulic diameter (1 to 2 mm). The channel may be smooth or micro-finned. Yang and Webb[1] and Webb and Yang[2] conducted condensation heat transfer tests using R-12 and R-134a in smooth (D_h=2.64 mm) and micro-finned (D_h=1.56 mm) flat tubes. They showed that the data were reasonably predicted by the Akers et al.[3] correlation. The data were underpredicted by the Shah[4] correlation. The heat transfer coefficients of the micro-finned tube were 10 to 60% higher than those of the smooth tube. The difference increased with increased vapor quality. They attributed the trend to the additional surface-tension drainage condensation on the fin surface, which is exposed to vapor at high vapor quality. Kim et al.[5] provided R-22 condensation data for the same flat tubes as those used by Yang and Webb.[1] They also confirmed the dominance of surface tension force at high vapor quality. Since the Montreal protocol, chlorofluorocar-bons (CFCs) and hydrochlorofluorocarbons (HCFCs) are being substituted by potential candidates. R-22, which has widely been used in household air-conditioners, is supposed to be replaced to R-410A or R-407C.

Despite the high condensing pressure, R-410A has negligible gliding temperature difference (less than 0.2 K), and has been given more attention compared to R-407C. However, the literature survey reveals no data on R-410A condensation in flat tubes. In this study, R-410A condensation tests were conducted in two different flat tubes; one with smooth inner surface (D_h= 1.41 mm), the other with micro-finned inner surface (D_h=1.56 mm). These are the same tubes tested by Yang and Webb[1] and Kim et al.[5] Cross-sectional photos of the tubes are shown in Fig. 1. The height and pitch of the micro-fin were 0.2 mm and 0.4 mm respectively. The test range covered the mass flux from 200 to 600 kg/m^{2}s and the heat flux from 5 to 15 kW/m^2. The saturation temperature was maintained at 45℃.

2. Experimental apparatus

A schematic drawing of the apparatus is shown in Fig. 2, and a detailed drawing of the test section is shown in Fig. 3. The apparatus and the test section were made similar to those used by Yang and Webb.[1] The test section comprises of a flat tube and an annular channel with a length of 455 mm. The refrigerant flows inside of the tube and the cooling water flows in the annular channel. For an accurate

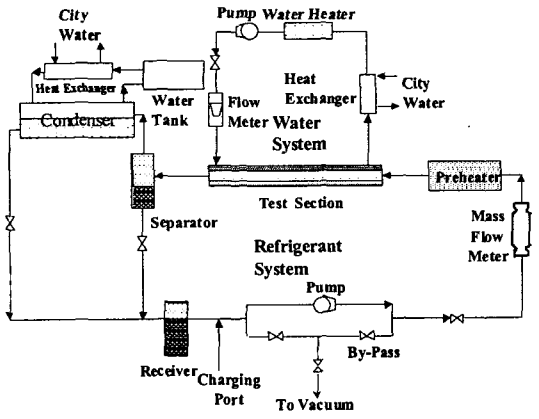

Fig. 2 Schematic drawing of the experimental apparatus.

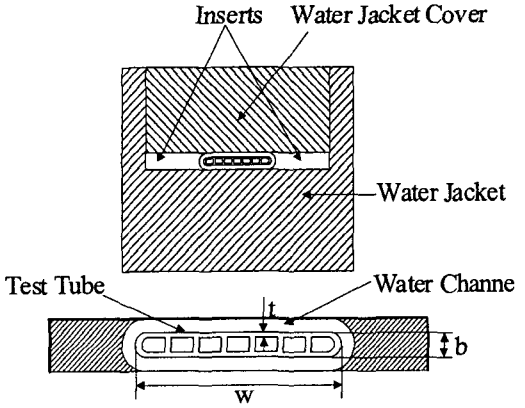

Fig. 3 Detailed drawing of the test section.

Table 1 Geometric details of the flat tubes and corresponding annular channels

		Micro-finned flat tube		Smooth flat tube	
	Item	Tube	Annulus	Tube	Annulus
Tube	w (mm)	16.00	18.00	18.00	20.30
	b (mm)	3.00	5.00	1.70	4.20
	A_c (mm)	22.68	39.60	14.72	51.58
	$A_i/L(P_w)$ (mm)	57.99	77.30	41.74	83.97
	D_h (mm)	1.56	2.05	1.41	2.46
	t (mm)	0.50	-	0.36	-
Fin	e (mm)	0.20	-	-	-
	p (mm)	0.40	-	-	-
	(deg)	40	-	-	-
	r_o (mm)	0.013	-	-	-
	r_b (mm)	0.15	-	-	-

measurement of tube-side condensation coefficient, it is important to minimize the thermal resistance of the annular side. This may be accomplished by increasing the annular-side water velocity. To increase the water velocity, the annular gap was maintained small (1.0 mm). Geometric details of the tested flat tubes and the corresponding annular channels are listed in Table 1.

As illustrated in Fig. 2, the refrigerant flows into the test section at a known quality and partly condenses in the test section by an annular-side cooling water. Two-phase refrigerant mixture from the test section enters the separator, where the liquid drains down to the receiver and the vapor flows into the upper shell-and-tube condenser. The condensed liquid drains down to the receiver. The sub-cooled liquid passes through the magnetic pump, mass flow meter, and enters the pre-heater. The refrigerant flow rate was controlled by by-passing an appropriate amount of liquid. The vapor quality into the test section was controlled by the heat input supplied to the pre-heater.

The heat flux to the flat tube was controlled by changing the temperature of a cooling water. The flow rate of the cooling water was fixed at 1.0 liter per minute throughout the test.

Temperatures were measured at five locations; refrigerant temperatures at inlet and outlet of the test tube, cooling water temperatures at inlet and outlet of the annular channel and a sub-cooled refrigerant temperature at the inlet of the pre-heater. Thermowells having five thermocouples each were used to measure local temperatures. Two absolute pressures were measured—one at the inlet of the test section, and the other at the inlet of the pre-heater. These absolute pressures were used to check the state (sub-cooled or saturated) of the refrigerant. A differential pressure transducer was used to measure the pressure drop across the test section. The saturation pressure corresponding to the saturation temperature 45℃ is 27 bar and the apparatus was checked for leak-tight. Leak tests were conducted by a soap bubble technique followed by a halogen leak detection. The leakage resulted in a decrease in pressure less than 0.5 kPa per hour. The condensation test started at the maximum heat flux and mass flux. After the system was stabilized, quality (from 0.1 to 0.9), heat flux (from 5 to 15 kW/m^2) and mass flux (from 200 to 600 kg/m^{2}s) were sequentially varied, all in a decreasing manner.

3. Data reduction

The tube-side condensation coefficient h_i is

determined from Eq. (1) using the overall heat transfer coefficient U_o and the annular-side heat transfer coefficient h_o. Here, A_m is the heat transfer area at the middle plane of tube wall.

$$h_i = \left[\left(\frac{1}{U_o} - \frac{1}{h_o}\right)\frac{A_i}{A_o} - \frac{tA_i}{tA_m}\right]^{-1} \quad (1)$$

The annular-side heat transfer coefficient h_o was determined from the modified Wilson plot as suggested by Farrell et al.[6] To run a Wilson plot test, it is important to maintain both the tube-side and the annular-side turbulent. To promote turbulence at the annular-side, thin wire of 0.3 mm diameter was wrapped around the tube at 3.0 mm pitch. The average vapor quality in the test tube is determined from Eq. (2).

$$x_{ave} = x_{in} - \Delta x/2 \quad (2)$$

Here, Δx is the change of vapor quality across the test section. The vapor quality into the test section is determined from Eq. (3). Here, Q_p is the heat supplied to the pre-heater and $T_{p,in}$ is the refrigerant temperature into the pre-heater.

$$x_{in} = \frac{1}{i_{fg}}\left[\frac{Q_p}{m_r} - c_{pr}(T_{sat} - T_{p,in})\right] \quad (3)$$

Experimental uncertainties were analyzed following the method by Kline and McClintock.[7] The uncertainty on the heat transfer coefficient ranged from 4.1% to 11.2%. The uncertainty increased as the vapor quality decreased.

4. Results and discussions

Fig. 4 shows the R-22 data by Kim et al.[5] Note that the actual wetted surface area was used for the heat transfer area. The micro-fin tube has 39% larger heat transfer area than the smooth tube. The micro-fin tube yields higher heat transfer coefficients, except at the high mass flux (600 kg/m^{2}s). At the mass flux 600 kg/m^{2}s, the heat transfer coefficients of both tubes are approximately the same.

The R-410A data are shown in Fig. 5. Similar to R-22, the micro-fin tube yields higher heat transfer coefficients at a low mass flux. At the high mass flux (600 kg/m^{2}s), however, the trend is reversed. The heat transfer coefficients of the smooth tube are higher. For R-22, both tubes yielded approximately the same heat transfer coefficients at G=600 kg/m^{2}s. Decrease of the heat transfer coefficient for finned tube has been reported by Carnavos[8] for single-phase turbulent flow. Fins act to reduce the flow velocity in the inter-fin region, and decrease the

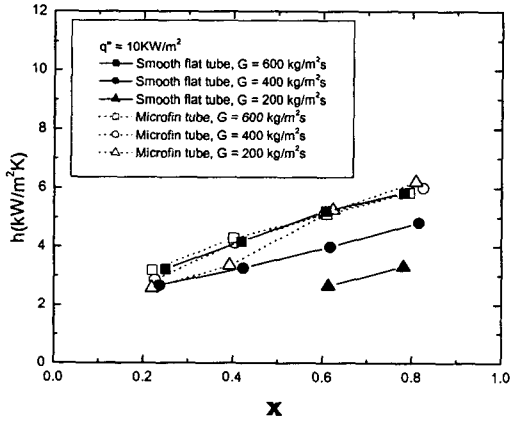

Fig. 4 R-22 condensation heat transfer coefficients.

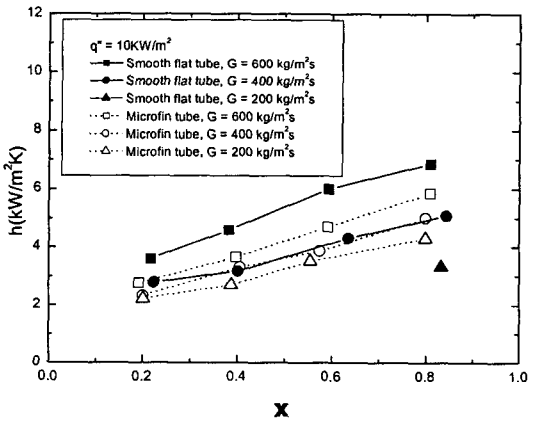

Fig. 5 R-410A condensation heat transfer coefficients.

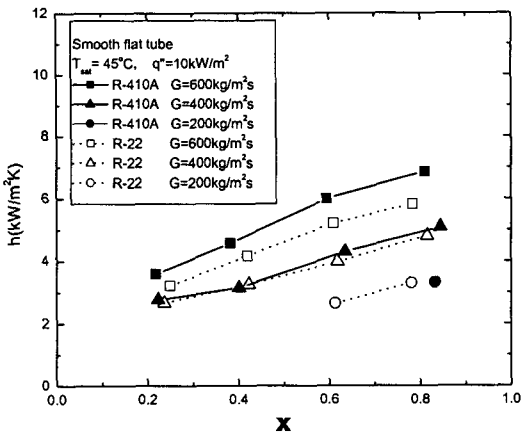

Fig. 6 Condensation heat transfer coefficients of R-22 and R-410A in the smooth tube.

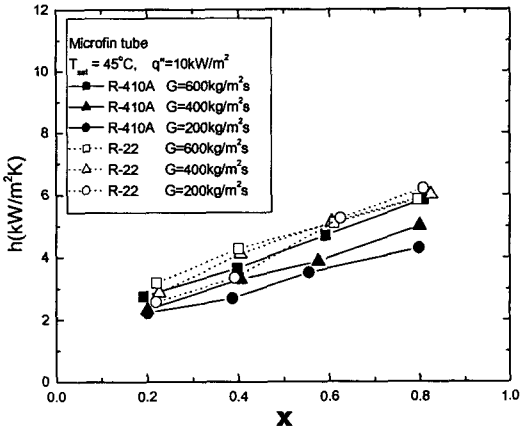

Fig. 7 Condensation heat transfer coefficients of R-22 and R-410A in the micro-fin tube.

heat transfer. For the condensation heat transfer, however, fins may induce the surface drainage force, and increase the heat transfer. At a low mass flux, where the reduction of the inter-fin velocity is likely to be small and the surface tension induced enhancement is considerable, finned tubes may yield higher heat transfer coefficients than the smooth tube. At a high mass flux, the reduction of the inter-fin velocity will be larger, and finned tubes may yield smaller heat transfer coefficients.

In Fig. 6, the heat transfer coefficients of R-410A are compared with those of R-22 for the smooth tube. The heat transfer coefficients of R-410A are slightly higher. The micro-fin data are compared in Fig. 7.

Different from the smooth tube, R-22 yields higher heat transfer coefficients. In addition, the R-22 data tend to converge irrespective of the mass flux at high qualities, whereas R-410A data do not show the converging characteristic. We may explain these results considering the thermal properties of the refrigerants. The higher heat transfer coefficients of R-410A for the smooth tube may be attributed to the larger thermal conductivity and smaller viscosity. Similar trends have been reported by Wijaya and Spatz[9] and Kwon et al.[10] for circular smooth tubes. To explain the micro-fin tube results, surface tension force should be considered in addition to the inertial force. The relative importance of the inertial force over the surface tension force may be obtained from the Weber number $[=G^2 D_h/(\rho_l \sigma)]$. Smaller Weber number implies stronger surface tension force. The Weber number of R-22 is 2.7 times smaller than that of R-410A at T_{sat}=45℃. Another reason could be larger ratio of specific vapor volume to specific liquid volume for R-22 (15.1 for R-22 as compared to 7.94 for R-410A). If a refrigerant has larger specific vapor volume, more fin area will be exposed to vapor for a given quality. The ratio of vapor-exposed fin area to total fin area has been calculated using the model by Yang and Webb,[11] and the results are shown in Fig. 8. Assuming a circular liquid-vapor interface and adopting Zivi's[12] void fraction model, Yang and Webb derived a simple equation for the flooded fraction of fin area. Fig. 8 indicates that, for R-22, more area is exposed to vapor at the same vapor quality. In addition, the exposition starts at a lower vapor quality. This may partly explain the high heat transfer coefficients of R-22 for the micro-fin tube. The mass flux independency for R-22 at high qualities (shown in Fig. 7) may also be attributed to the strong surface tension force. If the surface tension drainage condensation domi-

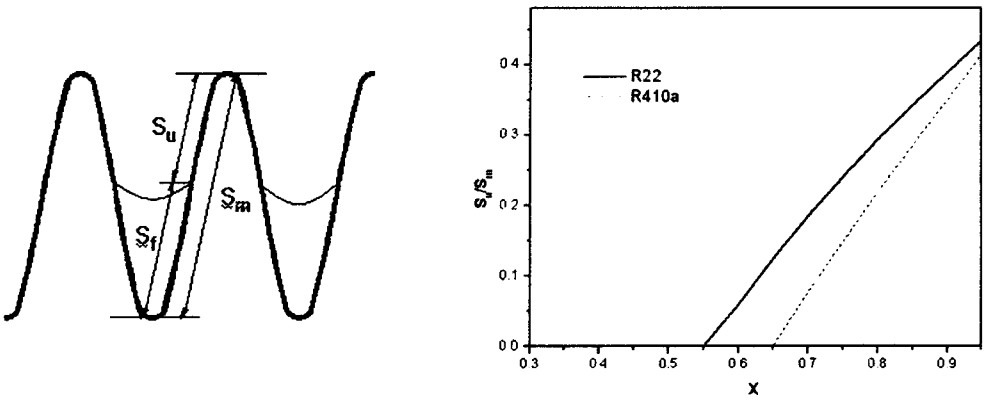

Fig. 8 The ratio of vapor-exposed fin area to total fin area calculated using Yang and Webb[11] model.

Table 2 Correlations cited in this study

Reference	Correlations
Akers et al.[3]	$\mathrm{Nu} = 0.0265\,\mathrm{Re}_{eq}^{0.8}\,\mathrm{Pr}_l^{1/3}$ $h = h_l\left[(1-x)^{0.8} + \frac{3.8x^{0.76}(1-x)^{0.04}}{P_{red}^{0.38}}\right]$ $h_l = 0.023\frac{k_l}{D_h}\,\mathrm{Re}_l^{0.8}\,\mathrm{Pr}_l^{0.4}$
Webb[14]	$h = h_l\left[1.31\,\mathrm{Pr}_l^{-0.185}(R^+)^A\,\mathrm{Re}_l^B\right]$ where $R^+ = 0.0994\,\mathrm{Re}_{eq}^{7/8}$ $A = 0.126\,\mathrm{Pr}_l^{-0.448}$ $B = -0.113\,\mathrm{Pr}_l^{0.563}$ $\mathrm{Re}_{eq} = \left[0.5\frac{D_h^3}{f_{l,eq}}\frac{\rho_l}{\mu_l^2}\left(\frac{dP}{dz}\right)_f\right]^{0.5}$ $f_{l,eq} = 0.079\,\mathrm{Re}_{eq}^{-0.25}$
Yang and Webb[11]	$h = h_u\frac{A_u}{A} + h_f\frac{A_f}{A}$ $h_f = 0.0265\frac{k_l}{D_h}\,\mathrm{Re}_{eq}^{0.8}\,\mathrm{Pr}_l^{1/3}$ $h_u = \sqrt{h_{sh}^2 + h_{sl}^2}$ $h_{sh} = 0.0265\frac{k_l}{D_h}\,\mathrm{Re}_{eq}^{0.8}\,\mathrm{Pr}_l^{1/3}$ $h_{st} = C\frac{\tau_z - \tau_i}{(dp/dz)}k_l\frac{(1/r_b)-(1/r_o)}{S_m}\frac{\mathrm{Re}_{eq}\mathrm{Pr}_l^{1/3}}{\mathrm{We}}$ $C = 0.0703$
This study (Modified Yang and Webb)	Smooth tube: Webbs[14] correlation Micro-fin tube: Same as Yang and webb[11] except $h_f = h_{sh} = h_{Webb}$

nates over the convective condensation, the heat transfer coefficients would be independent of the mass flux. Tang et al.[13] also showed that the heat transfer coefficients of R-22 are higher than those of R-410A for a circular axial micro fin tube.

The literature survey reveals that the state-of-the-art condensation correlation applicable to small diameter multi-channel tubes is that by Webb.[14] He extended the equivalent Reynolds number model by Moser et al.[15] by incorporating the Friedel[16] pressure drop correlation modified to small diameter tubes. Webb's correlation is provided in Table 2.

The present R-22 and R-410A data obtained from the smooth flat tube are compared with Webb's correlation in Fig. 9. Data are also compared with two other correlations Akers et al.[3] and Shah[4] which are generally accepted for condensation in round tubes with diameters larger than 7 mm. Fig. 9 shows that the data are well predicted by Webb's correlation (within ±30%). Akers et al. correlation slightly underpredicts the data and Shah correlation overpredicts the data. For the micro-fin tube at low quality, where fins are submerged below the liquid film, the heat transfer mechanism will be similar to that of the smooth tube as suggested by Yang and Webb.[11] Thus, the low quality micro-fin data ($x<0.65$ for R-410A and $x<0.55$ for R-22 based on the results from Fig. 8) are also compared with the correlations.

Fig. 9 shows that the results are similar to those of the smooth tube. Webb's correlation adequately predicts the data. Akers et al.'s correlation underpredicts and Shah's correlation overpredicts the data. This suggests that, as long as fins are submerged below the liquid film, smooth tube correlations may be equally successful to micro-fin tubes. One may consider the reduction of flow velocity in the inter-fin region for a more rational model.

For the micro-fin tube at high quality, where fins are exposed to vapor, the surface tension

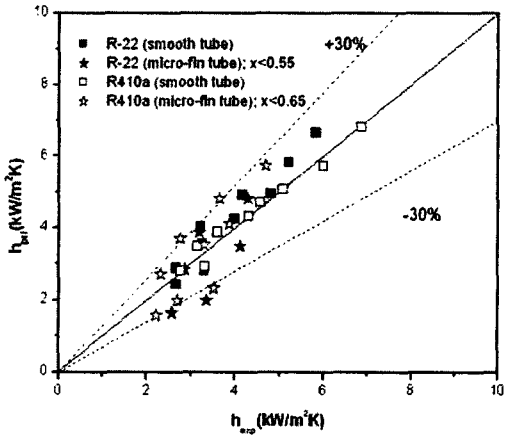

(a) Webb[14]

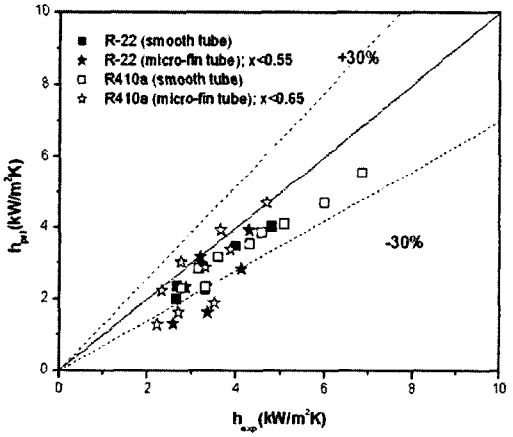

(b) Akers et al.[3]

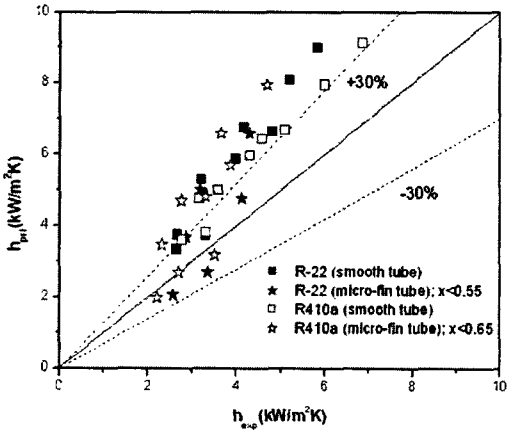

(c) Shah[14]

Fig. 9 Comparison of the smooth and micro-fin tube data with correlations.

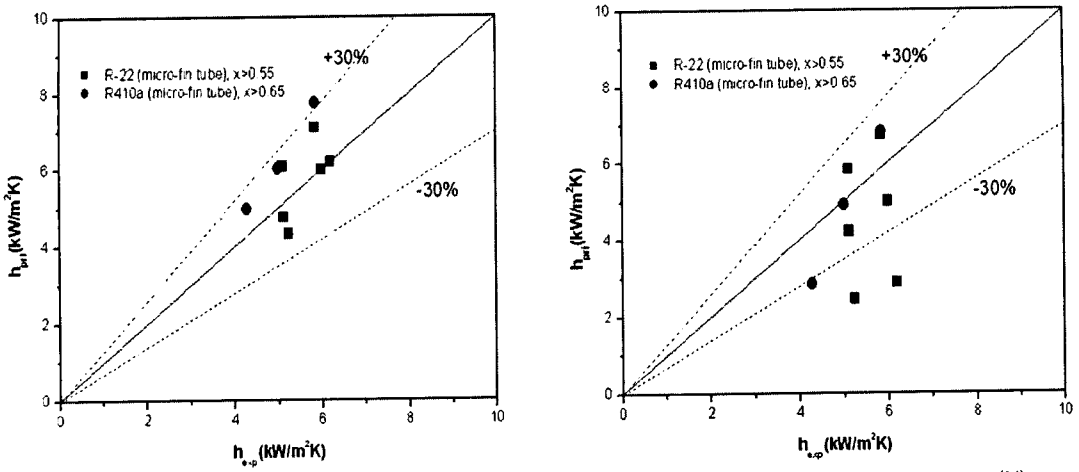

(a) Present model (modified Yang and Webb) (b) Smooth tube correlation (Webb[14])

Fig. 10 High quality micro-fin data compared with the present model and the smooth tube correlation.

term should be considered in addition to the vapor shear term in developing a correlation. Yang and Webb[11] developed a semi-empirical model, which can predict the condensation coefficient in micro-fin tubes. The Yang and Webb model is listed in Table 2. Detailed description of the model is described in Yang and Webb.[11] They proposed that condensation in a smooth tube or in a micro-fin tube at low vapor quality would be controlled by vapor shear. For a micro-fin tube at high quality, where both the vapor shear and the surface tension would be important, they proposed a model which combines the two forces in an asymptotic form. For the accurate prediction of surface tension controlled heat transfer, however, the shape of liquid film, which is dependent on the fin profile, should be known. This requires a solution of complex differential equations, which is only possible by a numerical approach. Yang and Webb, instead, assumed a linear surface tension drainage force, and then introduced a correction factor, which they obtained from data-fit. Yang and Webb proposed Akers et al. correlation to predict the vapor shear term (h_{sh}). The present study, however, has shown that Webbs[14] correlation is more appropriate, and thus has been adopted instead. The micro-fin data at high qualities ($x \geq 0.65$ for R-410A and $x \geq 0.55$ for R-22) were predicted by the present (modified Yang and Webb) model, and the results are shown in Fig. 10. As mentioned, Yang and Webb introduced a correction factor C to adjust the model and the data. The present model, however, do not need the correction factor. The present model is also listed in Table 2.

Fig. 10 shows that the present model predicts the data within ±30%. To check the applicability of a smooth tube correlation to a micro-fin tube when fins are exposed to vapor, the high quality data are compared with Webb's correlation. Fig. 10 reveals that the prediction is poor, and especially the R-22 data are highly underpredicted. This is expected because R-22 induces strong surface tension force, and accordingly yields high heat transfer coefficients.

5. Conclusions

Condensation heat transfer coefficients of R-410A were measured in a smooth and a micro-fin flat tube, and compared with those of R-22. Test range covered the mass flux from 200 to

600 kg/m^{2}s and the heat flux from 5 to 15 kW/m^2. The saturation temperature was 45℃. Listed below are major findings.

(1) The effect of surface tension drainage on the fin surface is more pronounced for R-22 than R-410A. The smaller Weber number for R-22 may be responsible.

(2) For the smooth tube, the heat transfer coefficient of R-410A is slightly larger than that of R-22. For the micro-fin tube, however, the reverse is true. Possible reason is provided considering physical properties of the refrigerants.

(3) For the smooth tube, Webb's correlation predicts the data reasonably well. For the micro-fin tube, the Yang and Webb model was modified to correlate the present data. The modified model predicts the data within ±30%.

Acknowledgements

Financial support from Sunmoon University (Regional Research Center for Advanced Climate Control Technology) is kindly acknowledged.

References

1. Yang, C. Y. and Webb, R. L., 1996, Condensation of R-12 in small hydraulic diameter extruded aluminum tubes with and without micro-fins, Int. J. Heat Mass Trans., Vol. 39, No. 4, pp. 791-800.
2. Webb, R. L. and Yang, C. Y., 1995, A comparison of R-12 and R-134a condensation inside small extruded aluminum plain and micro-fin tubes, C4961053195, IMechE, pp. 77-86.
3. Akers, W. W., Deans, H. A. and Crosser, O. K., 1959 Condensation heat transfer within horizontal tubes, Chem. Eng. Progress Symp. Series, Vol. 55, No. 29, pp. 171-176.
4. Shah, M. M., 1979, A general correlation for heat transfer during film condensation in tubes, Int. J. Heat Mass Transfer, Vol. 22, No. 4, pp. 547-556.
5. Kim, N. H., Cho, J. P. and Kim, J. O., 2000, R-22 condensation in flat aluminum multi-channel tubes, J. Enhanced Heat Transfer, Vol. 7, pp. 427-438.
6. Farrell, P., Wert, K. and Webb, R. L., 1991, Heat transfer and friction characteristics of turbulator radiator tubes, SAE Technical Paper Series 910197.
7. Kline, S. J. and McClintock, F. A., 1953, The description of uncertainties in single sample experiments, Mechanical Engineering, Vol. 75, pp. 3-9.
8. Carnavos, T. C., 1979, Cooling air in turbulent flow with internally finned tubes, Heat Transfer Engineering, Vol. 1, No. 2, pp. 41-46.
9. Wijaya, A. and Spatz, M. W., 1994, Two-phase flow condensation heat transfer and pressure drop characteristics, Proceedings of 1994 International Refrigeration Conference at Purdue, pp. 305-310.
10. Kwon, J. T., Park, S. K. and Kim, M. H., 2000, Enhanced effect of a horizontal micro-fin tube for condensation heat transfer with R22 and R410A, J. Enhanced Heat Transfer, Vol. 7, pp. 97-107.
11. Yang, C. Y. and Webb, R. L., 1997, A predicted model for condensation in small hydraulic diameter tubes having axial micro-fins, J. Heat Trans., Vol. 119, pp. 776-782.
12. Zivi, S. M., 1964, Estimation of steady state steam void fraction by means of principle of minimum entropy production, J. Heat Trans., Vol. 86, pp. 237-252.
13. Tang, L., Ohadi, M. M. and Johnson, A. T., 2000, Flow condensation in smooth and micro-fin tubes with HCFC-22, HFC-134a and HFC-410A refrigerants, J. Enhanced Heat Transfer, Vol. 7, pp. 289-310.
14. Webb, R. L., 1998, Prediction of condensation and evaporation in micro-fin and micro-channel tubes, In: Kakac, S., Bergles, A. E., Mayinger, F. and Yuncu, H., editors, Heat

transfer enhancement of heat exchangers: Kluwer Academic Publishers, pp. 529-550.
15. Moser, K., Webb, R. L. and Na, B., 1998, A new equivalent Reynolds number model for condensation in smooth tubes, J. Heat Trans., Vol. 120, pp. 410-417.
16. Friedel, L., 1979, Improved friction pressure drop correlations for horizontal and vertical two phase pipe flow, Paper E2, Europian Two Phase Flow Group Meeting, Ispra, Italy.